International Journal of Stem Cells Vol. 5, No. 2, 2012

ORIGINAL ARTICLE

Tissue Regeneration and Stem Cell Distribution in Adriamycin Induced Glomerulopathy

Maha Baligh Zickri[1], Marwa Mohamed Abdel Fattah[2], Hala Gabr Metwally[3]

[1]*Histology Department, Faculty of Medicine, Cairo University,* [2]*Misr University of Science and Technology,* [3]*Clinical Pathology Department, Faculty of Medicine, Cairo University, Cairo, Egypt*

Background and Objectives: Glomerulosclerosis develops secondary to various kidney diseases. It was postulated that adriamycin (ADR) induce chronic glomerulopathy. Treatment combinations for one year did not significantly modify renal function in resistant focal segmental glomerulosclerosis (FSGS). Recurrence of FSGS after renal transplantation impacts long-term graft survival and limits access to transplantation. The present study aimed at investigating the relation between the possible therapeutic effect of human mesenchymal stem cells (HMSCs), isolated from cord blood on glomerular damage and their distribution by using ADR induced nephrotoxicity as a model in albino rat.
Methods and Results: Thirty three male albino rats were divided into control group, ADR group where rats were given single intraperitoneal (IP) injection of 5 mg/kg adriamycin. The rats were sacrificed 10, 20 and 30 days following confirmation of glomerular injury. In stem cell therapy group, rats were injected with HMSCs following confirmation of renal injury and sacrificed 10, 20 and 30 days after HMSCs therapy. Kidney sections were exposed to histological, histochemical, immunohistochemical, morphometric and serological studies. In response to SC therapy multiple Malpighian corpuscles (MC) appeared with patent Bowman's space (Bs) 10 and 20 days following therapy. One month following therapy no remarkable shrunken glomeruli were evident. Glomerular area and serum creatinine were significantly different in ADR group in comparison to control and SC therapy groups.
Conclusions: ADR induced glomerulosclerosis regressed in response to cord blood HMSC therapy. A reciprocal relation was recorded between the extent of renal regeneration and the distribution of undifferentiated mesenchymal stem cells.

Keywords: Mesenchymal stem cells, Cord blood, Glomerulosclerosis, Adriamycin

Introduction

Drug induced glomerular injury was reported (1). It was postulated that adriamycin (ADR) induce chronic glomerulopathy. The latter is characterized by progressive glomerulosclerosis (2). Glomerulosclerosis develops also secondary to various kidney diseases including diabetic nephropathy and atherosclerosis (3).

Accepted for publication October 2, 2012
Correspondence to **Maha Baligh Zickri**
Histology Department, Faculty of Medicine, Cairo University, Cairo, Egypt
Tel: +2/0123955078, Fax: +0020235381183/+0020235381760
E-mail: mahakaah@yahoo.com

Treatment combination of cyclosporine and mycophenolate mofetil for one year did not significantly modify the evolution of renal function in resistant focal segmental glomerulosclerosis (FSGS) (4). The treatment of idiopathic FSGS patients with nephrotic syndrome is still unresolved and clinicians are faced with a challenge in producing response in the patient and slowing or halting the evolution towards kidney failure (5). Recurrence of FSGS after renal transplantation impacts long-term graft survival and limits access to transplantation. Immunosuppressive regimen had no effect on recurrence of FSGS (6).

Mesenchymal stem cells (MSCs) are stromal cells that have the ability to self-renew and exhibit multilineage differentiation. MSCs can be isolated from a variety of tissues, such as umbilical cord, bone marrow and adipose

tissue. The multipotent properties of MSCs make them an attractive choice for possible development of clinical applications (7). Cord blood transplant (CBT) has been widely used as an alternative source of mesenchymal cell support for stem cell transplant patients (8).

The present study aimed at investigating the relation between the possible therapeutic effect of HMSCs, isolated from cord blood on glomerular damage and their distribution. This was accomplished by using ADr induced nephrotoxicity as a model in albino rat.

Materials and Methods

Thirty three male albino rats weighing 150～200 g were used and divided into 3 groups placed in separate cages in the Animal House of Kasr El Aini. The rats were treated in accordance with guidelines approved by the Animal Use Committee of Cairo University.

Control group: 2 control rats, 1 for each experimental group. Each animal received single IP injection of distilled water.

Group A (ADR group): 16 rats, each received single (9) IP injection (10) of 5 mg/kg (11) ADR (Pharmacia Italia SPA, Nerviano, Italy) dissolved in distilled water. One rat was sacrificed thirty days following the day of injection for confirmation of renal damage. The remaining rats were subdivided into: Subgroups (A1), (A2) and (A3), in each subgroup 5 animals were sacrificed 10, 20 and 30 days following the confirmation of renal damage respectively.

Group S (SC therapy group): 15 rats received ADR by the same route, at the same frequency of administration and at the same dose as in the previous group. They were injected with 0.5 ml of cultured and labeled HMSCs suspended in phosphate buffer saline (PBS) in the tail vein (12). The injection was performed on two successive days following confirmation of renal damage. Stem cells were isolated from cord blood (13). Cord blood collection was performed at the Gynaecology Department, Faculty of Medicine, Cairo University. Stem cell isolation, culture and labeling were performed at Hematology Unit, New Kasr El Aini Teaching Hospital.

The rats were subdivided into: Subgroups S1, S2 and S3, in each subgroup 5 rats were sacrificed 10, 20 and 30 days following SC therapy.

Before sacrifice, blood was collected from eyes of animals using capillary tubes for assessment of serum creatinine in Clinical Pathology Department, Faculty of Medicine Cairo University.

Cord blood collection (14)

The storage and transport temperature was 15～22°C, transport time was 8～24 hours, sample volume was 65～250 ml, and no sample had signs of coagulation or hemolysis.

Mononuclear cell fraction isolation (14)

The mononuclear cell fraction (MNCF) was isolated by carefully loading 30 ml of whole blood onto 10 ml of Ficoll density media (Healthcare Bio-Sciences) in 50 ml polypropylene tubes. Centrifuge for 30 minutes at room temperature at 450×g and the interphase collected after aspirating and discarding the supernatant. The interphase was washed with 20 ml PBS and centrifuged at 150×g for 5 minutes at room temperature. The supernatant was aspirated and the cells were washed with PBS a second time. The cells were re-suspended in the isolation media to prevent adherence of monocytic cells. The isolation media was low-glucose DMEM (Dulbecco's modified Eagles medium) (Cambrex Bio Science, Minnesota, USA), penicillin (100 IU/ml) (Invitrogen), streptomycin (0.1 mg/ml) (Invitrogen), and ultraglutamine (2 mM) (Cambrex Bio-Science). Incubation was at 38.5°C in humidified atmosphere containing 5% CO_2.

Culture (14)

The isolation media were replaced after overnight incubation (12～18 hours) in order to remove non-adherent cells. The media were replaced every 3 days until MSC colonies were noted. The cultures were inspected daily for formation of adherent spindle-shaped fibroblastoid cell colonies. Sub-culturing was done by chemical detachment using 0.04% trypsin. Later, when cell numbers allowed, expansion was done in 25 cm^2 or 75 cm^2 tissue culture flasks.

Labeling (15)

Mesenchymal stem cells were labeled by incubation with ferumoxides injectable solution (25 microgramFe/ml, Feridex, Berlex Laboratories) in culture medium for 24 hours with 375 nanogram/ml poly L lysine added 1 hour before cell incubation. Labeling was histologically assessed using Prussian blue. Feridex labeled MSCs were washed in PBS, trypsinized, washed and resuspended in 0.01 Mol/L PBS at concentration of 1×1,000,000 cells/ml.

Cell viability analysis

Cell viability was done using trypan blue dye exclusion test. This method is based on the principle that viable cells do not take up certain dyes, whereas dead cells do.

Flow cytometry (16)

Flow cytometric analyses were performed on a Fluorescence Activated Cell Sorter (FACS) flow cytometer (Coulter Epics Elite, Miami, FL, USA). HMSC were trypsinized and washed twice with PBS. A total number of 1×10^5 HMSC were used for each run. To evaluate the HMSC marker profile, cells were incubated in 100 μl of PBS with 3 μl of CD105-FITC for 20 min at room temperature. Antibody concentration was 0.1 mg mL^{-1}. Cells were washed twice with PBS and finally diluted in 200 μl of PBS. The expression of surface marker was assessed by the mean fluorescence. CD105 (mesenchymal stem cell marker), CD133 (early hematopoietic & endothelial progenitor stem cell marker) and CD45 (panleucocytic marker) were also used. The percentage of cells positive for CD 105 was determined by subtracting the percentage of cells stained non-specifically with isotype control antibodies.

The rats were sacrificed using lethal dose of ether. Median abdominal incision was performed, both kidneys were excised and fixed in 10% formol saline for 24 hours. Paraffin blocks were prepared and 5 μm thick sections were subjected to the following studies.

Histological study

Hematoxylin and eosin (H&E) stain (17).

Histochemical study

Prussian blue (Pb) stain (18) for demonstration of iron oxide labeled therapeutic stem cells.

Immunohistochemical study

CD105 immunostaining (19) the marker for HMSCs. 0.1 ml prediluted primary antibody (CD105) rabbit polyclonal Ab (ab27422) and incubate at room temperature in moist chamber for 30-60 minutes. Tonsil used as positive control specimens. Cellular localization is the cell membrane. On the other hand, one of the lung sections was used as a negative control by passing the step of applying the primary antibody.

Morphometric study

Using Leica Qwin 500 LTD image analysis, assessment of the glomerular area using interactive measurements menu was done in 10 low power fields. The area% of Pb+ve cells and that of CD105+ve cells were estimated in the renal cortex. The measurments were done in 10 high power fields.

Statistical analysis (20)

Quantitative data were summarized as means and standard deviations and compared using one-way analysis-of-variance (ANOVA). p-values <0.05 were considered statistically significant. Calculations were made on SPSS software.

Results

Haematoxylin and eosin (H&E) stained sections

Control sections of cortex revealed normal structure (Fig. 1). In subgroup A1, some fields recruited occasional corpuscles with completely obliterated Bowman's space

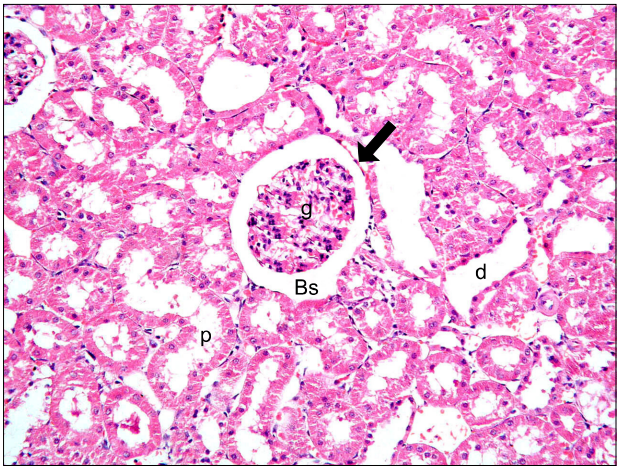

Fig. 1. Malpighian renal corpuscle containing a glomerulus (g), Bowman's space (Bs), parietal layer of Bowman's capsule (arrow), proximal convoluted tubules (PCT) (p) and distal convoluted tubules (DCT) (d) in control group (renal cortex; H&E, ×200).

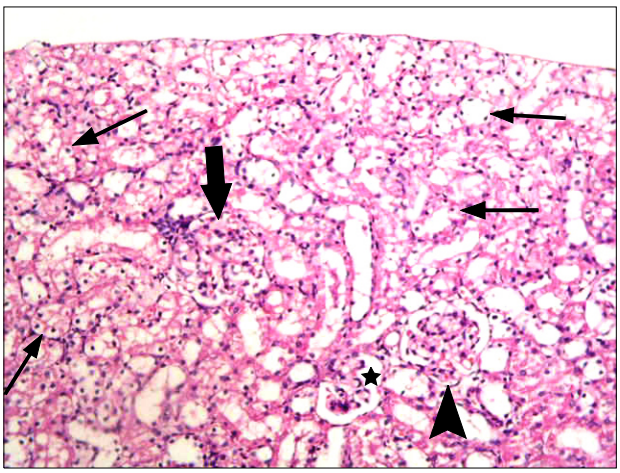

Fig. 2. A corpuscle with completely obliterated Bs (thick arrow), a second with partially obliterated space (arrowhead) and a third with patent space (*). Note vacuolated cytoplasm and dark nuclei (thin arrows) of the cells lining multiple cortical tubules in subgroup A1 (renal cortex; H&E, ×200).

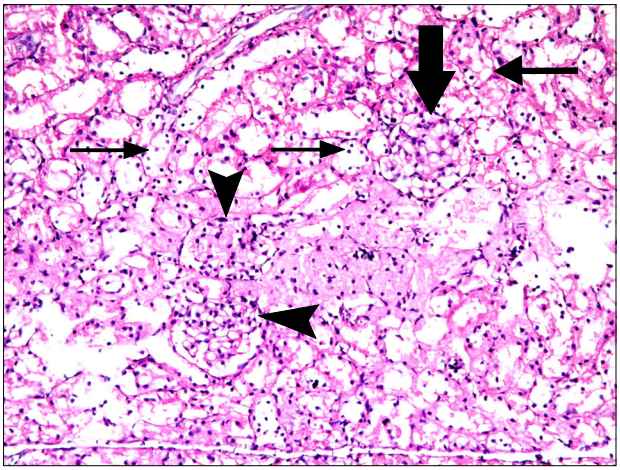

Fig. 3. A corpuscle with completely obliterated Bowman' space (thick arrow) and two corpuscles with partially obliterated spaces (arrowheads). Note vacuolated cytoplasm and dark nuclei (thin arrows) of the cells lining multiple cortical tubules in subgroup A2 (renal cortex; H&E, ×200).

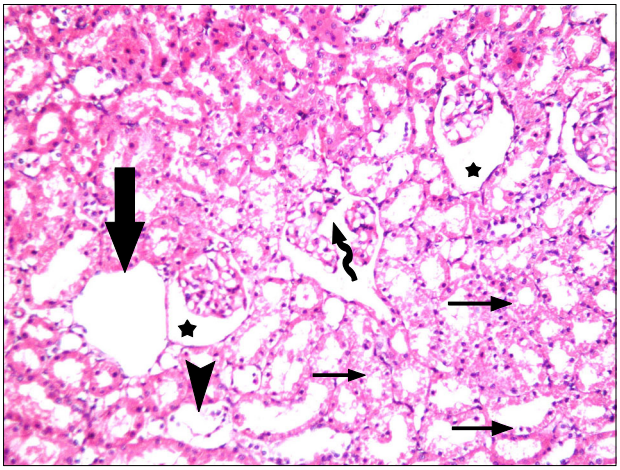

Fig. 4. Two corpuscles with shrunken glomeruli and wide Bowman' space (*). Note a corpuscle with separated glomerular loops (curved arrow), empty space lined by squamous cells (thick arrow), vacuolated cytoplasm of the cells lining multiple cortical tubules (thin arrows) and detached epithelial lining (arrowhead) of a cortical tubule in subgroup A3 (renal cortex; H&E, ×200).

(Bs) and others with partially obliterated space. Vacuolated cytoplasm and dark nuclei were noticed in the cells lining multiple cortical tubules (Fig. 2). In subgroup A2, corpuscles with completely obliterated Bs and some others with partially obliterated spaces were seen in multiple fields. Vacuolated cytoplasm and dark nuclei of the cells lining multiple cortical tubules were evident (Fig. 3). Subgroup A3 demonstrated corpuscles with shrunken glomeruli and wide Bs, others with separated glomerular loops. Occasional empty spaces lined by squamous cells

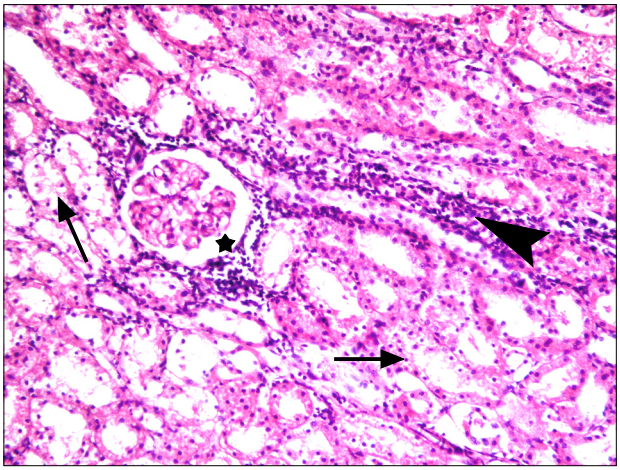

Fig. 5. A corpuscle with patent space (*). Vacuolated cytoplasm and dark nuclei (thin arrows) of the cells lining few cortical tubules are seen. Note mononuclear infiltration (arrowhead) in subgroup S1 (renal cortex; H&E, ×200).

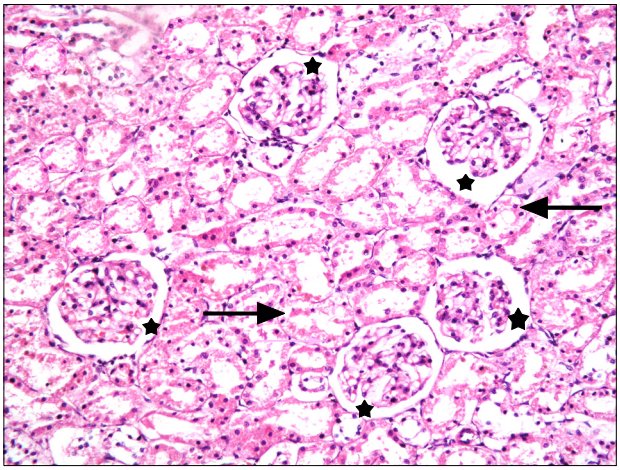

Fig. 6. Five corpuscles with patent space (*). Note vacuolated cytoplasm and dark nuclei (thin arrows) of the cells lining few cortical tubules in subgroup S2 (renal cortex; H&E, ×200).

were noticed. In addition, vacuolated cytoplasm and dark nuclei of the cells lining multiple tubules and detached epithelial lining were found in occasional cortical tubules (Fig. 4).

In subgroup S1 and S2, multiple corpuscles with patent space were obvious. Vacuolated cytoplasm and dark nuclei of the cells lining few cortical tubules were seen. Mononuclear infiltrating cells were noticed in some fields (Figs. 5, 6). In subgroup S3 no remarkable shrunken glomeruli were evident. Vacuolated cytoplasm and dark nuclei were noticed in the cells lining few cortical tubules (Fig. 7).

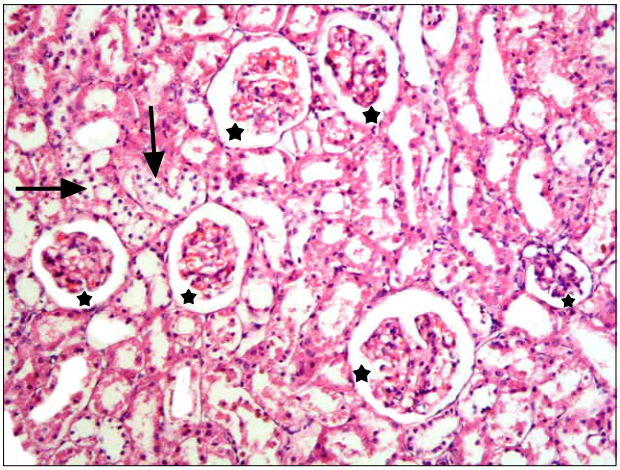

Fig. 7. Six corpuscles with patent Bowman's space (*) and few tubules with vacuolated cytoplasm and dark nuclei of the lining cells (thin arrows) in subgroup S3. Sections in the renal cortex showing (renal cortex; H&E, ×200).

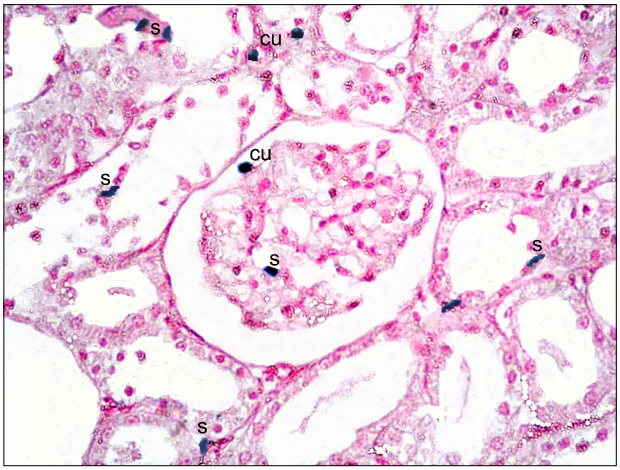

Fig. 9. Multiple spindle (s) and few cuboidal (cu) Pb+ve cells in peritubular capillaries and among the epithelial lining of CT in subgroup S1 (renal cortex; Prussian blue, ×400).

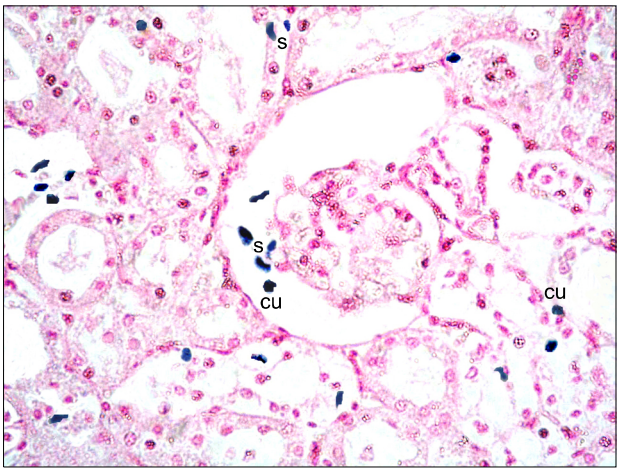

Fig. 8. Multiple spindle (s) and few cuboidal (cu) Pb+ve cells at the glomerulus, in the Bs and at the epithelial lining of the cortical tubules in subgroup S1 (renal cortex; Prussian blue, ×400).

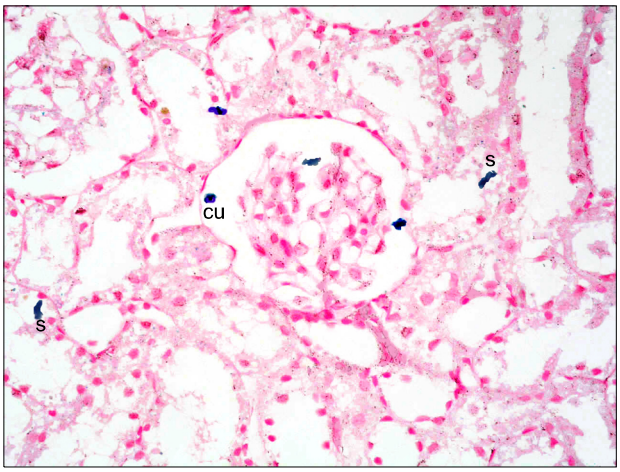

Fig. 10. Two cuboidal (cu) and fewer spindle (s) +ve cells at the glomerulus, in the Bs and at the lining epithelial cells of the cortical tubules in subgroup S3 (renal cortex; Prussian blue, ×400).

Prussian blue stained sections

Subgroup S1 revealed multiple spindle and few cuboidal Pb positive (+ve) cells at the glomeruli, in the Bs and at the epithelial lining of the cortical tubules (Fig. 8). While, subgroup S2 recruited some spindle and few cuboidal +ve cells at the glomeruli and at the epithelial lining of the cortical tubules compared to subgroup S1 (Fig. 9). Subgroup S3 showed few spindle +ve cells at the lining epithelial cells of the cortical tubules compared to subgroups S1and S2 (Fig. 10).

CD105 immunostained sections

Subgroup S1 showed +ve CD105 immunoexpression in multiple cortical tubules. The reaction appeared granular in spindle cells (Figs. 11, 12). Subgroup S2 demonstrated +ve immunostaining in fewer cortical tubules compared to subgroup S1 (Fig. 13). Subgroup S3 revealed +ve reaction in fewer cortical tubules compared to subgroups S1and S2 (Fig. 14).

Morphometric results

The mean glomerular area denoted a significant difference ($p<0.05$) in subgroups A2 and A3 compared to control and other experimental subgroups (Table 1, Fig. 15). Statistical analysis indicated a significant increase ($p<0.05$) in the mean area% of PB +ve and CD105 +ve cells

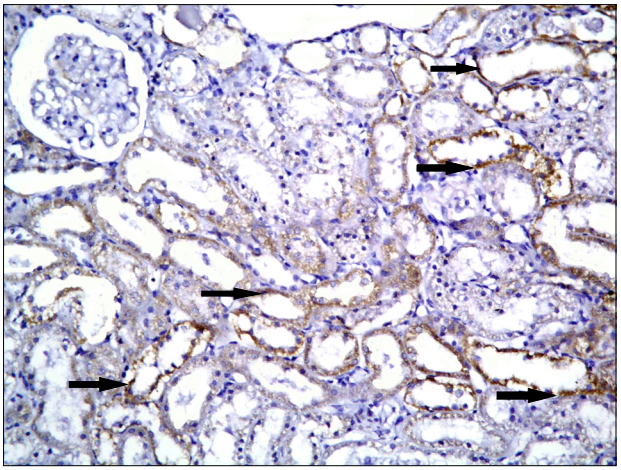

Fig. 11. +ve immunostaining in multiple cortical tubules (arrows) in subgroup S1 (CD105, ×200).

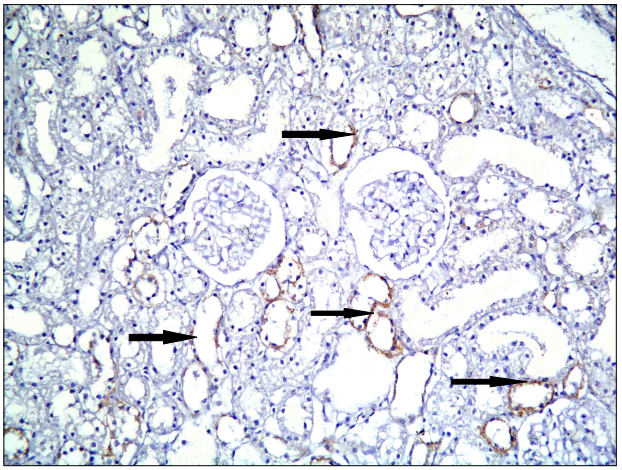

Fig. 13. +ve immunostaining in fewer cortical tubules (arrows) in subgroup S2 compared to Fig. 11 (CD105, ×200).

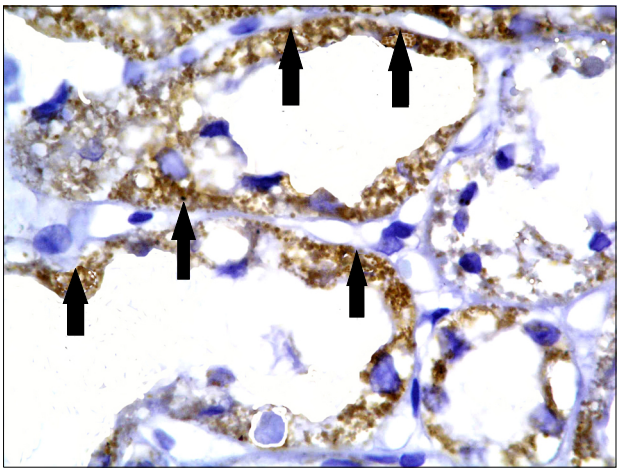

Fig. 12. Higher magnification of the previous figure showing granular reaction in multiple spindle cells (arrows) among the lining of cortical tubules (CD105, ×1,000).

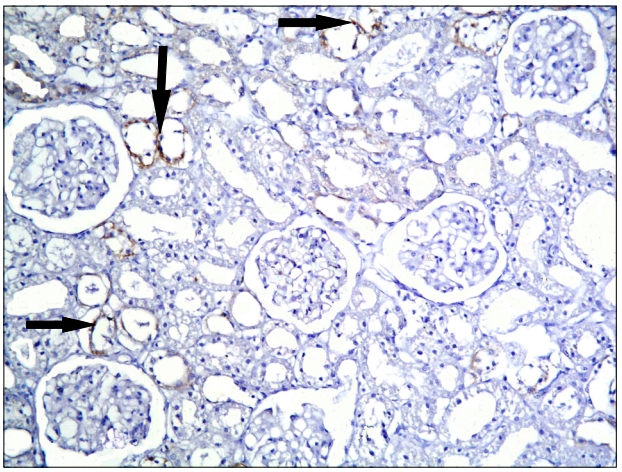

Fig. 14. +ve immunostaining in fewer cortical tubules (arrows) compared to Figs. 11 and 13 in subgroup S3 (CD105, ×200).

in subgroup S1 compared to S2 and S3. A significant difference ($p<0.05$) was also recorded between subgroups S2 and S3 (Table 1, Figs. 16, 17).

Serological results

A significant increase ($p<0.05$) in the mean value of serum creatinine was detected in ADR subgroups in comparison to SC therapy subgroups (Table 1, Fig. 18).

Discussion

The current study demonstrated ameliorating effect of cord blood HMSC therapy on ADR induced glomerular damage. ADR being a commonly used chemotherapeutic drug, as evidenced by Dai et al. (21) was used as a model for induced nephropathy in albino rat. This was evidenced by histological, histochemical, immunohistochemical, morphometric and serological studies.

Concerning changes in the MRCs, in subgroup A1 some corpuscles with completely obliterated Bs and some others with partially obliterated space were found. While in subgroup A2, multiple corpuscles with completely and partially obliterated Bs were detected. The latter findings were confirmed by a significant increase in the mean glomerular area in subgroup A2. It could be commented that ADR induced oxidative stress resulted in morphological changes in the MRC. Coresh et al. (22) related glomerular distension to FSGS, an early pathologic feature of many

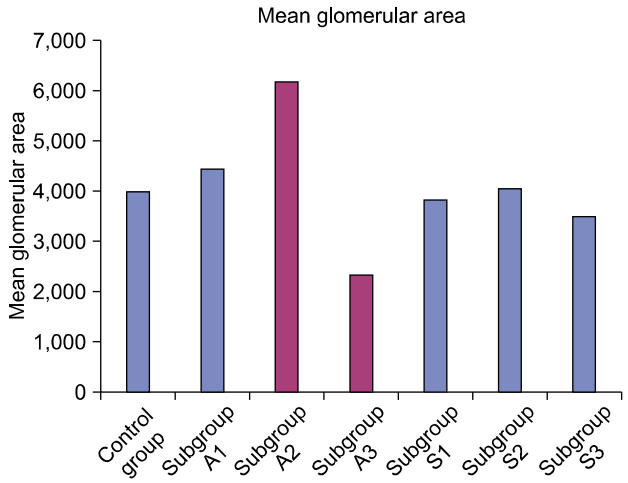

Fig. 15. Mean glomerular area in control and experimental groups.

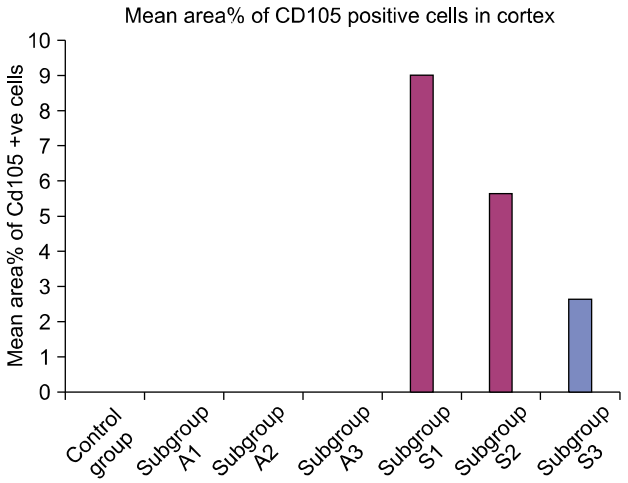

Fig. 17. Mean area% of CD105 positive cells in control and experimental groups.

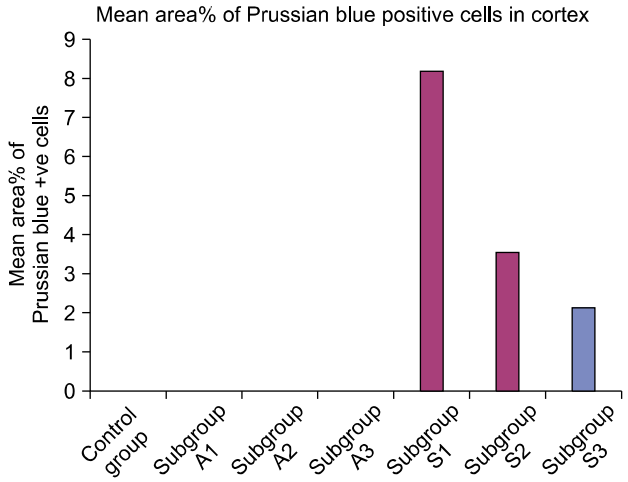

Fig. 16. Mean area% of Prussian blue positive cells in control and experimental groups.

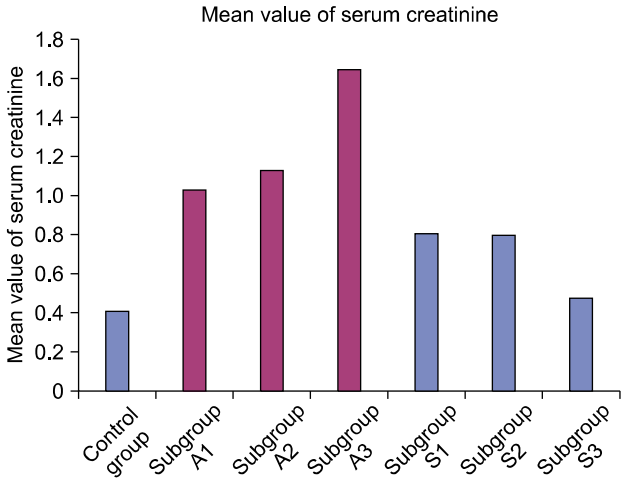

Fig. 18. Mean value of serum creatinine in control and experimental groups.

common forms of chronic kidney diseases. The resulting end-stage kidney failure that necessitates renal replacement therapy is growing annually, this poses a challenge to the medical community. Viscomi et al. (23) referred FSGS to effects of angiotensin II on mesangial cell growth. Cao et al. (24) stated that in ADR nephropathy model, a single dose of ADR produces loss of podocyte foot process architecture, progressive podocyte depletion that initiate glomerulosclerosis and nephropathy.

Subgroup A3 demonstrated corpuscles with shrunken glomeruli and wide Bs, others with separated glomerular loops. These changes were confirmed by a significant decrease in the mean glomerular area compared to control and the other subgroups. Occasional empty spaces lined by squamous cells were noticed. This change might be correlated to disappearance of the glomerular loops following glomerular atrophy, leaving empty Malpighian corpuscle surrounded by the parietal layer of the Bowman's capsule. In addition, it was reported that ADR induced glomerular structural damage (25).

Vacuolated cytoplasm and dark nuclei were noticed in the cells lining multiple cortical tubules in all ADR subgroups. In addition, in subgroup A3 detached epithelial lining was found in occasional cortical tubules. These effects were confirmed by G2-phase cell cycle arrest due to DNA damage by ADR (26). It was commented that the introduction of DNA breaks and inhibition of religation of the broken DNA strands are contributing factors. Lipid peroxidation was also described.

The mean value of serum creatinine was significantly

Table 1. Mean±standard deviation (SD) of glomerular area, area% of Prussian blue +ve cells, area% of CD105 +ve cells and serum creatinine in control and experimental groups

Groups and subgroups	Glomerular area	Area% of Pb+ve cells	Area% of CD105 +ve cells	Serum creatinine
Control group	3997.48±12.04	–	–	0.4100
Subgroup A1	4453.83±284.41	–	–	1.0300[d]
Subgroup A2	6174.18±224.40[a]	–	–	1.1360[d]
Subgroup A3	2329.88±308.03[a]	–	–	1.6420[d]
Subgroup S1	3833.19±254.64	8.16±0.17[b]	9.01±0.81[b]	0.8140
Subgroup S2	4067.99±176.15	3.49±0.39[c]	5.63±0.43[c]	0.7960
Subgroup S3	3493.10±496.92	2.09±0.35	2.59±0.32	0.7600

[a]Significant compared to group 1 and subgroups A1, S1, S2 and S3, [b]significant compared to subgroups S2 and S3, [c]significant compared to subgroup S3, [d]significant compared to group 1, subgroups S1, S2 and S3.

increased in ADR group which may denote impairment of renal function. It was proved that oxidative stress augments urea and creatinine levels in serum and albumin excretion in urine (27) and impaired renal function was confirmed on injection of doxorubicin 10 mg/kg in rats (28). The extent of glomerulosclerosis and mesangial expansion in ADR nephrosis were not modified by medical treatment in rat (29). This point is controversial.

Concerning changes in the MRC, subgroup S1 showed corpuscles with patent space. Subgroup S2 demonstrated multiple corpuscles with patent space. In subgroup S3 no remarkable shrunken glomeruli were seen. Morphometry confirmed comparable mean glomerular area to the control group. It was investigated whether BM derived SCs were responsible for rescue of renal disease by being an alternative to lifelong dependence on dialysis (30).

Vacuolated cytoplasm and dark nuclei of the cells lining fewer cortical tubules ere seen in subgroups S1, S2 and S3 in comparison to subgroups A1, A2 and A3 respectively. Chen et al. (31) commented on effectiveness and safety of adipose derived MSC treatment in preserving renal parenchymal integrity from ischemic injury.

In S1 subgroup, multiple spindle and few cuboidal Pb +ve cells were found at the glomeruli, in the Bs and at the epithelial lining of the cortical tubules. The +ve cells were fewer in subgroup S2 and fewest in subgroup S3. The previous findings were confirmed by a significant increase in the mean area % of +ve cells in subgroup S1. In accordance, MSC were described as attractive candidates for renal repair, because nephrons are of mesenchymal origin and stromal cells are of crucial importance for signaling. The potential of MSC for renal repair was reported intravenously and by intrarenal injection into mice (32).

In subgroup S1, multiple spindle CD105+ve immunostained cells were evident among the lining epithelium of multiple cortical tubules. Recently, nephron regeneration and repair of glomerulonephritis were reviewed by adipose-derived mesenchymal stem cells (33). Umbilical cord blood (UCB) is a reasonable option for the treatment of patients with hereditary BM failure syndromes. In patients given an unrelated UCB transplantation, only cord blood units containing a high number of cells should be considered to improve the results (34).

In the present study, a significant decrease in the level of serum creatinine was noted in SC therapy subgroups compared to ADR subgroups. Recently, transplantation of pluripotent SCs appears to improve serum indices of liver function and survival rate in mice after CCl4-induced hepatic damage (35).

In conclusion

ADR induced renal damage was represented by glomerulosclerosis that progressed into glomerular atrophy. The morphological findings were confirmed by morphometric assessment and correlated to progressive deterioration of the renal function manifested as progressive elevation of serum creatinine. Cord blood HMSC therapy proved definite amelioration of the glomerular and serological changes. A reciprocal relation was recorded between the extent of renal regeneration and the distribution of undifferentiated mesenchymal stem cells.

Potential conflict of interest

The authors have no conflicting financial interest.

References

1. Gautier JC, Riefke B, Walter J, Kurth P, Mylecraine L, Guilpin V, Barlow N, Gury T, Hoffman D, Ennulat D, Schuster K, Harpur E, Pettit S. Evaluation of novel bio-

markers of nephrotoxicity in two strains of rat treated with Cisplatin. Toxicol Pathol 2010;38:943-956
2. Jiao YQ, Yi ZW, He XJ, Liu XH, He QN, Huang DL. Does injection of metanephric mesenchymal cells improve renal function in rats? Saudi J Kidney Dis Transpl 2011;22:501-510
3. Sasaki M, Shikata K, Okada S, Miyamoto S, Nishishita S, Kataoka HU, Sato C, Wada J, Ogawa D, Makino H. The macrophage is a key factor in renal injuries caused by glomerular hyperfiltration. Acta Med Okayama 2011;65:81-89
4. Segarra Medrano A, Vila Presas J, Pou Clavé L, Majó Masferrer J, Camps Doménech J. Efficacy and safety of combined cyclosporin A and mycophenolate mofetil therapy in patients with cyclosporin-resistant focal segmental glomerulosclerosis. Nefrologia 2011;31:286-291
5. Rivera Hernández F. How to treat corticosteroid-resistant idiopathic focal segmental glomerulosclerosis? Nefrologia 2011;31:247-250
6. Sharief S, Mahesh S, Del Rio M, Telis V, Woroniecki RP. Recurrent focal segmental glomerulosclerosis in renal allograft recipients: role of human leukocyte antigen mismatching and other clinical variables. Int J Nephrol 2011;2011: 506805
7. Ding DC, Shyu WC, Lin SZ. Mesenchymal stem cells. Cell Transplant 2011;20:5-14
8. Maurer MH. Proteomic definitions of mesenchymal stem cells. Stem Cells Int 2011;2011:704256
9. Zickri M, Refaat N and Abdl Wahab N. Histological and immunohistochemical study on the effect of alpha-tocopherol (vitamin E) on doxorubicin (adriamycin) induced nephrotoxicity in albino rat. The 27th Scientific Conference of the Egyptian Society of Histology and Cytology 2003.
10. Zhu J, Zhang J, Xiang D, Zhang Z, Zhang L, Wu M, Zhu S, Zhang R, Han W. Recombinant human interleukin-1 receptor antagonist protects mice against acute doxorubicin-induced cardiotoxicity. Eur J Pharmacol 2010;643: 247-253
11. Lee VW, Qin X, Wang Y, Zheng G, Wang Y, Wang Y, Ince J, Tan TK, Kairaitis LK, Alexander SI, Harris DC. The CD40-CD154 co-stimulation pathway mediates innate immune injury in adriamycin nephrosis. Nephrol Dial Transplant 2010;25:717-730
12. Lee YG, Hwang JW, Park SB, Shin IS, Kang SK, Seo KW, Lee YS, Kang KS. Reduction of liver fibrosis by xenogeneic human umbilical cord blood and adipose tissue-derived multipotent stem cells without treatment of an immunosuppressant. Tissue Engineering and Regenerative Medicine 2008;5:613-621
13. Stocum DL, Zupanc GK. Stretching the limits: stem cells in regeneration science. Dev Dyn 2008;237:3648-3671
14. Koch TG, Heerkens T, Thomsen PD, Betts DH. Isolation of mesenchymal stem cells from equine umbilical cord blood. BMC Biotechnol 2007;7:26
15. Kraitchman DL, Heldman AW, Atalar E, Amado LC, Martin BJ, Pittenger MF, Hare JM, Bulte JW. In vivo magnetic resonance imaging of mesenchymal stem cells in myocardial infarction. Circulation 2003;107:2290-2293
16. Haasters F, Prall WC, Anz D, Bourquin C, Pautke C, Endres S, Mutschler W, Docheva D, Schieker M. Morphological and immunocytochemical characteristics indicate the yield of early progenitors and represent a quality control for human mesenchymal stem cell culturing. J Anat 2009; 214:759-767
17. Kiernan JA. Histological and Histochemical methods: Theory and Practice. 3rd ed. London New York and New Delhi: Arnold Publisher; 2001. 111-162
18. Ellis R. Perls Prussian blue Stain Protocol, Pathology Division, Queen Elizabeth Hospital: South Australia: 2007
19. Yagi H, Soto-Gutierrez A, Navarro-Alvarez N, Nahmias Y, Goldwasser Y, Kitagawa Y, Tilles AW, Tompkins RG, Parekkadan B, Yarmush ML. Reactive bone marrow stromal cells attenuate systemic inflammation via sTNFR1. Mol Ther 2010;18:1857-1864
20. Emsley R, Dunn G, White IR. Mediation and moderation of treatment effects in randomised controlled trials of complex interventions. Stat Methods Med Res 2010;19:237-270
21. Dai C, Stolz DB, Kiss LP, Monga SP, Holzman LB, Liu Y. Wnt/beta-catenin signaling promotes podocyte dysfunction and albuminuria. J Am Soc Nephrol 2009;20:1997-2008
22. Coresh J, Selvin E, Stevens LA, Manzi J, Kusek JW, Eggers P, Van Lente F, Levey AS. Prevalence of chronic kidney disease in the United States. JAMA 2007;298:2038-2047
23. Viscomi C, Spinazzola A, Maggioni M, Fernandez-Vizarra E, Massa V, Pagano C, Vettor R, Mora M, Zeviani M. Early-onset liver mtDNA depletion and late-onset proteinuric nephropathy in Mpv17 knockout mice. Hum Mol Genet 2009;18:12-26
24. Cao Q, Wang Y, Zheng D, Sun Y, Wang Y, Lee VW, Zheng G, Tan TK, Ince J, Alexander SI, Harris DC. IL-10/TGF-beta-modified macrophages induce regulatory T cells and protect against adriamycin nephrosis. J Am Soc Nephrol 2010;21:933-942
25. Tang SC, Leung JC, Chan LY, Eddy AA, Lai KN. Angiotensin converting enzyme inhibitor but not angiotensin receptor blockade or statin ameliorates murine adriamycin nephropathy. Kidney Int 2008;73:288-299
26. Papeta N, Zheng Z, Schon EA, Brosel S, Altintas MM, Nasr SH, Reiser J, D'Agati VD, Gharavi AG. Prkdc participates in mitochondrial genome maintenance and prevents Adriamycin-induced nephropathy in mice. J Clin Invest 2010;120:4055-4064
27. Abo-Salem OM, El-Edel RH, Harisa GE, El-Halawany N, Ghonaim MM. Experimental diabetic nephropathy can be prevented by propolis: Effect on metabolic disturbances and renal oxidative parameters. Pak J Pharm Sci 2009;22: 205-210
28. Boutabet K, Kebsa W, Alyane M, Lahouel M. Polyphenolic fraction of Algerian propolis protects rat kidney against acute oxidative stress induced by doxorubicin. Indian J Nephrol 2011;21:101-106
29. Sun W, Zhu Z, Yu J, Wang YH, Xiong M, Gao X, Zhao ZH, Liu XG. Effects of Chinese herbal medicine Huaiqi-

huang Granule on nephrin and podocin expressions in renal tissues of rats with adriamycin-induced nephrosis. Zhong Xi Yi Jie He Xue Bao 2011;9:546-552
30. Sugimoto H, Mundel TM, Sund M, Xie L, Cosgrove D, Kalluri R. Bone-marrow-derived stem cells repair basement membrane collagen defects and reverse genetic kidney disease. Proc Natl Acad Sci U S A 2006;103:7321-7326
31. Chen YT, Sun CK, Lin YC, Chang LT, Chen YL, Tsai TH, Chung SY, Chua S, Kao YH, Yen CH, Shao PL, Chang KC, Leu S, Yip HK. Adipose-derived mesenchymal stem cell protects kidneys against ischemia-reperfusion injury through suppressing oxidative stress and inflammatory reaction. J Transl Med 2011;9:51.
32. Kunter U, Rong S, Djuric Z, Boor P, Müller-Newen G, Yu D, Floege J. Transplanted mesenchymal stem cells accelerate glomerular healing in experimental glomerulonephritis. J Am Soc Nephrol 2006;17:2202-2212
33. Otto WR, Wright NA. Mesenchymal stem cells: from experiment to clinic. Fibrogenesis Tissue Repair 2011;4:20.
34. Bizzetto R, Bonfim C, Rocha V, Socié G, Locatelli F, Chan K, Ramirez O, Stein J, Nabhan S, Miranda E, Passweg J, de Souza CA, Gluckman E; Eurocord and SAA-WP from EBMT. Outcomes after related and unrelated umbilical cord blood transplantation for hereditary bone marrow failure syndromes other than Fanconi anemia. Haematologica 2011;96:134-141
35. Jin SZ, Liu BR, Xu J, Gao FL, Hu ZJ, Wang XH, Pei FH, Hong Y, Hu HY, Han MZ. Ex vivo-expanded bone marrow stem cells home to the liver and ameliorate functional recovery in a mouse model of acute hepatic injury. Hepatobiliary Pancreat Dis Int 2012;11:66-73